Available online at www.sciencedirect.com
SCIENCE DIRECT
International Journal of Mass Spectrometry 251 (2006) 1–9
International Journal of Mass Spectrometry
www.elsevier.com/locate/ijms

Secondary ion emission from condensed CO bombarded by fission fragments

L.S. Farenzena [a], R. Martinez [a], P. Iza [a], C.R. Ponciano [a], M.G.P. Homem [b], A. Naves de Brito [b], E.F. da Silveira [a,*], K. Wien [1]

[a] *Departamento de Física, Pontifícia Universidade Católica, 22543-970 Rio de Janeiro RJ, Brazil*
[b] *Laboratório Nacional de Luz Síncrotron, Box 6192, 13084-971 Campinas SP, Brazil*

Received 4 July 2005; received in revised form 21 October 2005; accepted 14 December 2005
Available online 23 January 2006

Abstract

Frozen CO was bombarded by ∼65 MeV fission fragments and the emitted secondary ions were analyzed by time-of-flight mass spectrometry. Target was kept at UHV conditions and its temperature was varied from 25 K up to complete sublimation of the ice film. The observed positive cluster ion series are well represented by the chemical expression $(CO)_mC_n^+$, where m and $n \geq 0$, and the negative ones by C_n^- and $(CO)_mO^-$. The positive cluster ion series with the highest desorption yield is $(CO)_2C_n^+$, in accordance with the particular high binding energy of $(CO)_2$. The total negative ion yield is about 90 smaller than the positive one (2.8 ions/impact) and the main negative ion series observed is C_n^-.

The desorption yields of the cluster ion series decrease exponentially with the mass of the cluster, and it is proposed that the decay constant, k_m, characterizes the process. The C_n^+ and C_n^- series have a fast decay ($k_m = 0.047\,u^{-1}$) and should be generated by fast gas-phase reactions in the thermalized nuclear track plasma. The $(CO)_m^+$ series presents a slow decay constant ($k_m = 0.007\,u^{-1}$); its members are probably residues of the fractured solid. Desorption yields depend weakly on target temperature up to near 30 K, when fast sublimation occurs.

Fullerene ions were not observed within $Y(C_{40}^+) \leq 2 \times 10^{-4}$ ions/impact.

Keywords: Secondary ions; Condensed gas; CO ice; Ion cluster; TOF SIMS; Temperature dependence

1. Introduction

Secondary ion (SI) emission from frozen gases bombarded by ^{252}Cf fission fragments (FF) have been studied by several researchers, e.g. [1–8]. Motivation for such studies comes from material science [1], molecular physics [2–5] and astrophysics [6–8]. The aim of the present work is to extend the analysis of SI emitted by frozen water [6] and by frozen CO_2 [7,8] to frozen CO. The bombardment of CO ice by keV ions and MeV light ions has also been studied, in particular by Chrisey et al. [9], Hudson and Moore [10] and Haring et al. [11]. Another dimension of cometary ice bombardment is occurring today (July 4th, 2005) inside the scope of the Deep Impact project.

Since the pioneering work of Macfarlane and Torgerson [12] it is known that high energetic heavy ions are capable of inducing desorption of organic molecules as intact species from organic solid targets. Usually, at masses below 100 u, the mass spectrum is dominated by (atomic or molecular) fragmentary ions and, above the molecular mass, often by cluster ions. Fast chemical reactions inside the nuclear track plasma can generate new compounds (see, for instance [7,8]), which may show up in the mass spectra as secondary ions.

The experiments were addressed to the mass spectra of pure CO; the spectra of contaminant H_2O are known from previous experiments [6]. The gas was condensed at the lowest possible temperature (∼25 K) and then bombarded by fission fragments during its warming up, producing electronic sputtering. In the following, the experimental method is described and then the experimental data obtained with pure CO are presented and discussed. So far, the secondary ion mass spectrum of frozen CO by electronic sputtering has not yet been published.

* Corresponding author. Tel.: +55 21 3114 1272; fax: +55 21 3114 1040.
E-mail address: enio@vdg.fis.puc-rio.br (E.F. da Silveira).
[1] Guest of the Institute of Nuclear Physics, Technical University, 64289 Darmstadt, Germany.

1387-3806/$ – see front matter © 2006 Elsevier B.V. All rights reserved.
doi:10.1016/j.ijms.2005.12.006

2. Experimental method

2.1. The ice target

The substrate for the condensed gases was a thin Au foil (thickness 0.51 μm, diameter 8 mm) mounted onto a Cu frame, which was connected to the cold finger of a helium closed-cycle cryostat system (Edwards Coldhead model 2/9). The temperature of the Cu frame was measured by means of a Copper-Constantan thermocouple, which has a sensitivity of 0.008 mV/K at 25 K. Thus, in this method, the accuracy of temperature measurement depends strongly on the value and stability of the reference temperature (ambient temperature of the voltmeter). The lowest temperature of the target foil achievable by means of the cryostat set-up was estimated to be 25 K. The target was surrounded by a Cu thermoshield having a temperature of about 50 K.

The ice layer was prepared by transporting CO in a stainless steel tube and blowing the gas slowly towards the target foil under an angle of 45° (see Fig. 1). In order to get a gross measure of the ice layer thickness, the energy loss ΔE_α of α particles passing the ice target was measured by means of a surface barrier detector mounted behind the target. The α particles – provided by 94% of the decay rate of a ^{252}Cf source (positioned at 17 mm in front of the target) – have the energy of 6.1 MeV. Energy loss tables (Northcliffe and Schilling [13]) were used to calculate the ice layer thickness from the measured ΔE_α. The lowest and the largest measurable thickness were about 60 nm and 7000 nm, respectively. Continuous measurements of ΔE_α during condensation allowed determining the growth rate of the ice layer. The flow rate of the gas stream was controlled by the partial pressure of CO inside the spectrometer chamber.

2.2. The TOF SIMS method and data acquisition

^{252}Cf fission fragments having energies of about 65 MeV (after passing the protection foil of the Cf source) were used for heavy ion bombardment of the ice target. The positive and negative SI emitted from the ice surface were measured by time-of-flight secondary ion mass spectrometry, TOF SIMS, (see, for instance, Wien [14]). As seen in the sketch shown in Fig. 1, the ^{252}Cf fission fragments penetrate the ice layer at the target's front side, from where the SI were backward ejected with respect to the incident projectiles and accelerated towards the stop detector, an assembly of two microchannel plates. The target potential could be set at +5 kV or −5 kV, depending on the desired SI charge for analysis. The quantity measured for each detected SI is the time it needs to fly from the target surface to the stop detector. Two different methods were simultaneously used to get a clean start signal for this time measurement. The start signal was generated by the detection of:

1. secondary electrons produced at the target's back side, which are accelerated to about 2 keV (detected by a second microchannel plate assembly);
2. the complementary fission fragment ejected from the Cf source in backward direction (detected by a third microchannel plate assembly).

The timing of the FF-signals is worse than that of the e^- signals mainly because of the wide fission fragment velocity distribution. However, this method allows the use of thick targets,—i.e. targets which cannot be traversed by the projectiles. In order to minimize the random events in the TOF spectra and to determine the true start rate (number of fission fragment impacts/s on the target), the FF signals were employed to gate the e^--start events. In the present experiments the true start rate was 120–160/s.

Start and stop signals were introduced into constant-fraction discriminators and then into a time-to-digital converter for producing spectra of the flight times, i.e. the TOF spectra. The mass spectra were obtained by considering that the SI mass is proportional to the square of TOF and by using an internal calibration. Such spectra were taken as a function of time, automatically stored in time intervals of 30 s or more seconds. As the target temperature was also monitored, the yield of certain secondary ions could be followed over a warming up period of hours.

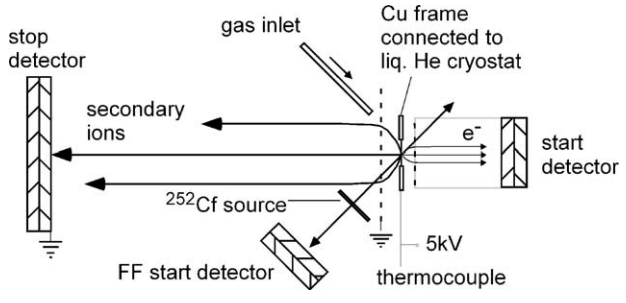

Fig. 1. Experimental setup used to analyze electronic sputtering: frozen gas targets were bombarded by ^{252}Cf fission fragments to produce secondary ions.

3. Secondary ion emission analysis

3.1. CO ice mass spectra

The TOF mass spectrum of positive secondary ions ejected from CO ice at a target temperature of about 25 K extends up to mass ∼1000 u and is partially shown in Fig. 2; for clarity, its low mass part ($m < 33$ u) is expanded in the insert. Several cluster ion series were identified: the series $(CO)_m$ occurs at the high mass part of the spectra, while the $(CO)_mC_n^+$ series dominates the intermediate region. The C_n^+ and $(CO)_mC_n^+$ series are better seen in Fig. 3a; the C_n^- series is observed in the negative secondary ion spectrum (Fig. 3b).

The contamination of the target surface was reduced by rest gas condensation: the sample was continuously refreshed by means of a steady CO gas stream onto the target. The growth rate of the CO ice layer was 0.2 nm/s. A spectrum measured after condensation with a definite ice layer thickness did not show essential differences, except that the relative intensity of rest gas ions has increased by one order of magnitude (see, for instance, H_2O^+ and H_3O^+ peaks in insert of Fig. 2 and in Fig. 3a).

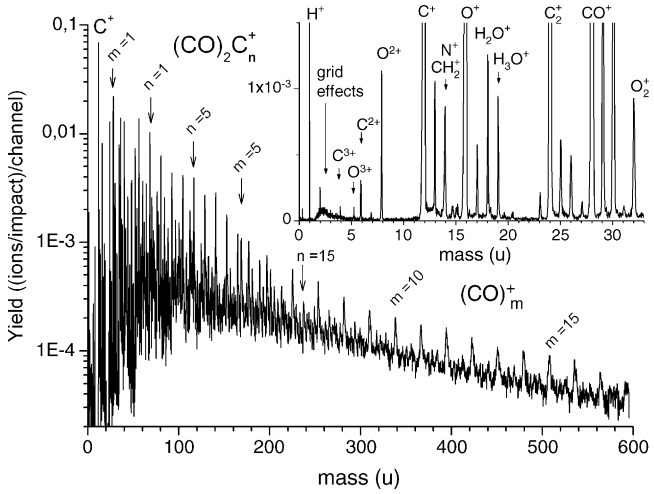

Fig. 2. TOF mass spectrum of positive secondary ions emitted from CO ice. The insert shows an expansion of the mass region below 33 u.

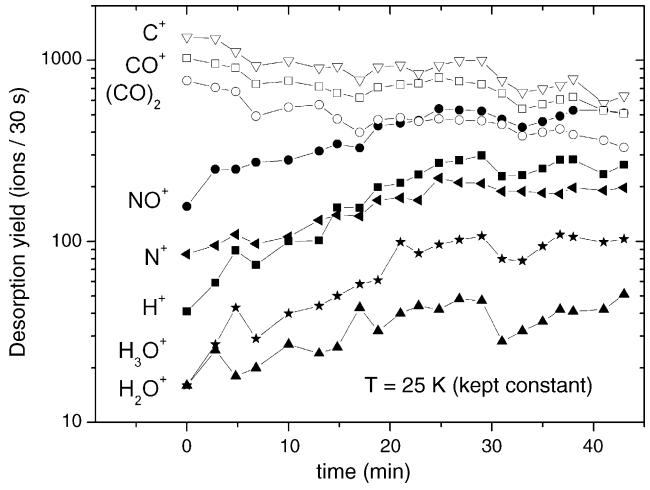

Fig. 4. Secondary ion yields of CO ice as a function of time at constant temperature $T = 25$ K. Open data symbols correspond to CO specific ions, closed data symbols to background ions.

The main residual gases were H_2O, N_2 and O_2. Since mass lines of CO specific ions should appear only at masses $m = 4(3i + 4j)$, with i and $j = 1, 2, 3, \ldots$, background ions with mass values in-between are easily identified.

In order to distinguish between CO specific ions and rest gas ions, the following procedure was employed: A fresh layer of CO ice was steadily condensed on the target at a temperature $T = 25$ K, until a thickness of about 200 nm was reached. Then, CO dosing was stopped and a series of 21 TOF measurements was started, each for 100 s. The intensity of well-resolved mass lines was then plotted versus the time of measurement. As seen in Fig. 4, within the 43 min of measurement the counting rate of, for instance, H_2O^+ increases by a factor of 7, and that of NO^+ by 2.3. CO specific ions such as CO^+ and $(CO)_2{}^+$ decrease by a factor of about 2.2, probably because their ionization, a very rare process [7], is overtaken by rest-gas contaminants of the target surface. At the beginning, the intensity of H^+ and other hydrogen containing ions such as H_2O^+ and H_3O^+ is remarkably low with respect to earlier studies of frozen gases [7,2]. The existence of nitrogen at the target surface is indicated by the N^+, NO^+ (see insert of Fig. 2) and CN^- (see Fig. 3b) signals.

3.2. Absolute yields of CO specific ions

The spectrum shown in Fig. 2 has been used to evaluate the absolute yields of the CO specific ions. The detection efficiency of the TOF spectrometer for ions ejected from the target by FF bombardment was determined with help of a frozen CO_2 target,—corresponding absolute ion yields were known from recent experiments [7] similar to those of the present study. The results for each positive ion species are presented as bar-spectra in Fig. 5; the negative ones are presented in Fig. 7. The total (integrated) positive and negative absolute ion yields are 2.78 and 0.031, respectively. Note that the ratio of these total yields

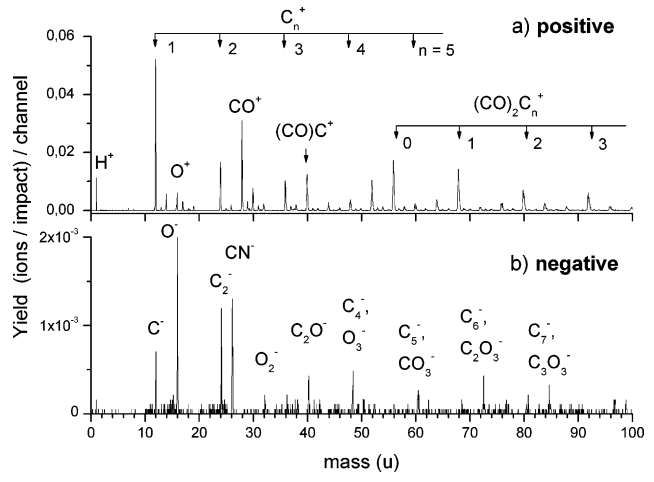

Fig. 3. TOF mass spectra of: (a) positive and (b) negative secondary ions emitted from CO ice at $T = 25$ K. The data were obtained during 500 s after condensation of a 200 nm thick CO ice layer.

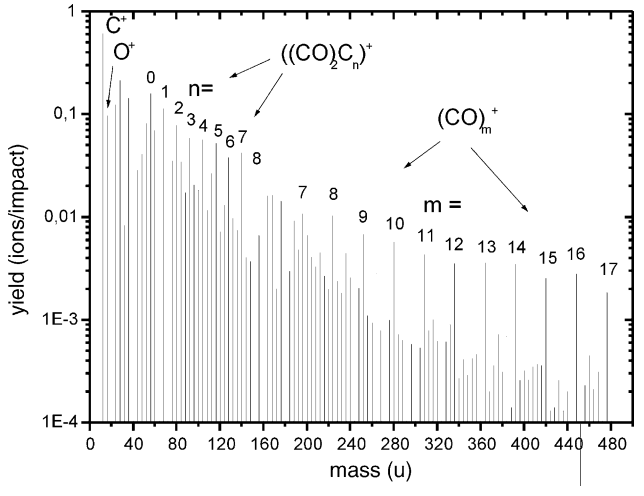

Fig. 5. Bar-spectrum of positive CO specific ions ejected from CO ice at $T = 25$ K. The series $(CO)_2C_n{}^+$ and $(CO)_m{}^+$ are labeled through the indexes m and n. Background has been subtracted.

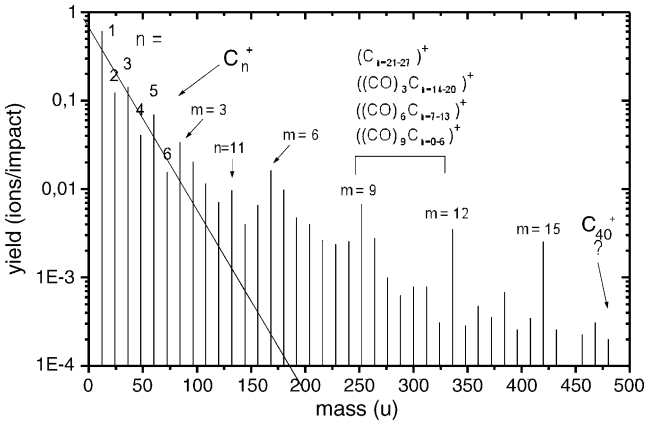

Fig. 6. Bar-spectrum of the first group of positive cluster ion series $(CO)_{m=3i}C_n^+$ and C_n^+. A decreasing exponential was fitted through the first 6 C_n^+ data points. At mass $m = 480$ u the position of the possible fullerene ion C_{40}^+ is marked. For further explanations, see text.

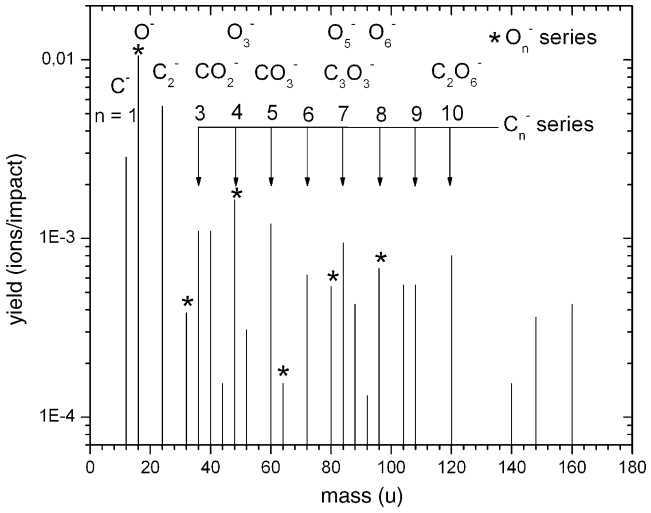

Fig. 7. Bar-spectrum of negative CO specific ions ejected from CO ice at $T = 25$ K. Yields are typically one or two orders of magnitude lower than the positive ones. The series C_n^- and O_n^- are labeled. The series C_n^- decreases exponentially on n, the fluctuations being due to the molecular structure of each component. Other possible series are $(CO)C_n^-$ and $(CO_2)O_n^-$.

is 90, much higher than the values reported in literature for CO_2 and H_2O [6,7].

The lines in the positive ion spectrum of frozen CO can be described by a single chemical expression:

$$(CO)_m C_n^+ \quad \text{with}$$

$$m = 0,\ 1,\ 2,\ 3,\ \ldots \text{ and } n = 0,\ 1,\ 2,\ 3,\ \ldots.$$

The SI, which are not described by the expression $(CO)_mC_n^+$, are O^+, O_2^+ and CO_2^+, holding only about 5% of the total yield. Actually, ions containing carbon clusters, C_n, dominate the spectrum, corresponding to 78% of the total yield.

3.3. Structure of the cluster series

3.3.1. Sorting the series according the cluster masses

The positive ion mass spectrum presented in Fig. 2 was reduced into the bar-spectrum shown in Fig. 5. Three cluster ion series are promptly identified: $(CO)_m^+$, C_n^+ and $(CO)_2C_n^+$, indicating that $(CO)_mC_n^+$ should be a more general structure for the observed secondary ions. Concerning the index m, this ensemble can be furthermore divided into three independent groups of cluster ion series, i.e. $m = 3i$, $3i+1$ and $3i+2$, so that each sequence of masses never overlaps the two others. These three groups are:

$$(CO)_{m=3i}C_n^+$$

$$(CO)_{m=3i+1}C_n^+$$

$$(CO)_{m=3i+2}C_n^+ \quad \text{with}$$

$$i = 0,\ 1,\ 2,\ 3,\ \ldots \text{ and } n = 0,\ 1,\ 2,\ 3,\ \ldots.$$

As an example, Fig. 6 presents the absolute ion yields measured for the $m = 3i$ group, i.e. that part of the whole spectrum which is composed of the series $(CO)_{m=3i}C_n^+$. The spectra of the other two groups look similar. As $(CO)_3$ has the same mass as C_7, a characteristic feature of each of these partial spectra is that no ambiguity between i and n exists for the first 6 (if $m = 0$) or 7 (if $m = 1$ or 2) members, implying that their yields can not be shared among them.

3.3.2. The exponential behavior of the yields

Its is clear from Figs. 5 and 6 that, in the range of non-overlapping, the yields of the 3 high-yield cluster series C_n^+, $(CO)C_n^+$, $(CO)_2C_n^+$ decrease exponentially as the cluster mass $m(n)$ increases, i.e. when the number of periodic constituents (the cluster nuclearity, n) increases. The slopes of the exponential decay for two of the three low-yield positive series of Fig. 6 and for the negative series C_n^- and $(CO_2)_n^-$ (see Fig. 7) are not as steep as the three high-yield series. Care should be taken when determining the decay constant (k) of the series, according to their dependence on m or on n. This behavior can be described by:

$$Y = Y_0\, e^{-k_m\, m(n)} = Y_{bh}\, e^{-k\, n} \tag{1}$$

where $m(n) = m_{bh} + m_c n$, m_{bh} is the band head mass and m_c the mass difference between two adjacent cluster members; therefore, $k = m_c k_m$. The quantity k is more suitable for discussions concerning stoichiometry (or probabilities of atomic rearrangement), while k_m is more appropriate for discussions on molecular dynamics because it involves secondary ion masses (accelerations, velocities and, therefore, different neutralization times). When the yield decrease is given by the sum of two exponentials, then k_m^F refers to the *f*ast decay one and k_m^S to the *s*low decay one.

The exponential dependence of the secondary ion cluster yield on the cluster nuclearity has been observed in many other experiments based on ion bombardment of ices (H_2O [6,18,19], CO_2 [7], NH_3 [20]) or on laser irradiation (e.g. [21]). Effusive cluster source (Knudsen Cell) generates such type of distribution in equilibrium conditions [22]. Some models also predict the exponential cluster behavior: the evaporative ensemble model of Bjørnholm and Klots [22], the quasi-equilibrium model of

de Heer and co-workers [22] and statistical models treating re-aggregation of individual atoms upon or after ejection [23–26].

3.3.3. C_n^+ and O_n^+ series

Inspection of Fig. 5 reveals exponential decreasing yields for masses $4n$, which allows ambiguous designation of the several C_iO_j series. The dominant peak at mass 12 u defines the band head of the $12n$-mass series, i.e. the C_n^+ one. The formation of C_n clusters requires the presence of unbound carbon in the nuclear track plasma. If dissociation of CO is the main process for producing unbound carbon, the nuclear track plasma should contain an equivalent amount of oxygen. On the other hand, the yield of O^+ is observed to be about six times smaller than that of C^+: this is probably because, in the hot track plasma, carbon atoms are preferentially ionized compared to the oxygen atoms, due to their smaller ionization potential (11.3 and 13.6 eV, respectively) and also because the electron affinity of O^- is higher than C^-. Moreover, since the reaction product O_n^+ exhibits a comparatively low yield, aggregation of free oxygen ions seems to be less likely than for carbon atoms in CO ice: one possible explanation could be the formation and emission of neutral O_2, O_3, and CO_2, forcing the oxygen cluster ion series to decrease faster than carbon series.

3.3.4. $(CO)_mC_n^+$ and $(CO)_m^+$ series

Neutral molecules may attach themselves to the reactive C_n^+ seed during the desorption phenomena. It should be expected that the abundant $(CO)_m$ bulk molecules do so, given rise to the $(CO)_mC_n^+$ ion series: mass lines at masses 40, 52, 64, 76, 88, 100 u for series $(CO)C_n^+$; masses 56, 68, 80, 92, 104, 116, 128 u for $(CO)_2C_n^+$.

The series $(CO)_mC_n^+$ overlap with other series for high values of n. This is illustrated in Fig. 6: up to $m = 72$ u, the spectrum displays the first 6 non-superimposed members of the C_n^+ series. Between the masses $m = 84$ u and 156 u, this series is superimposed with the series $(CO)_3C_n^+$. With increasing mass, more and more series overlap. The actual complexity of such multi superimposing is marked for the mass range 252–324 u: here, four series overlap; their designations are given in Fig. 6. To evaluate the spectral contributions of each series in this selected mass range is hardly possible, but extrapolation of the trend of yields towards the next band head (marked by $m = 12$) allows the determination of the yield of $(CO)_{12}^+$. This procedure was applied to all band heads $(CO)_m^+$, including the data of the other two partial spectra. The resulting yields of the series $(CO)_m^+$ are plotted versus mass in Fig. 8.

As already seen in Fig. 6, at high masses, the $(CO)_m^+$ series exhibits a relatively slow decrease of ion yields with mass, which can be described by an exponential decay curve $Y = Y_0 \exp(-k_m m)$, with the decay constant $k_m = 0.007\ u^{-1}$. The yields of the first two members of the $(CO)_m^+$ series do not fit to this exponential decay, the yields are one order of magnitude higher than expected. The ions CO^+ and $(CO)_2^+$ are formed by a process different from that for the $(CO)_m^+$ series, as will be discussed in Section 4. In Fig. 8, this slowly decreasing yield curve is compared with the corresponding yield curves of the

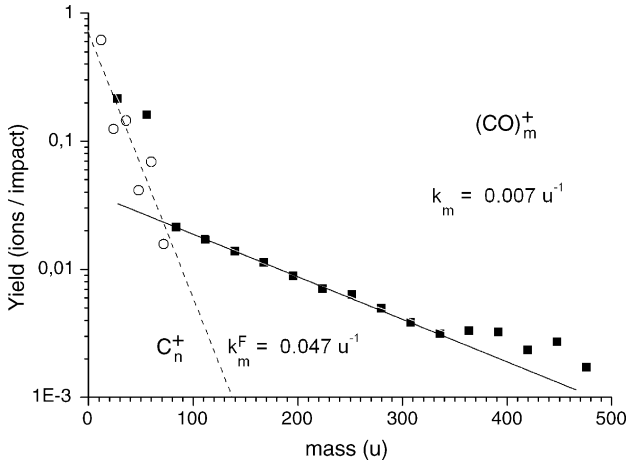

Fig. 8. Cluster yields of the C_n^+ and $(CO)_mC_n^+$ series, plotted as functions of the cluster nuclearity, n. The slope of their exponential decay gives the value of the decay constant, k.

ion series C_n^+. An exponential decay curve has been fitted to the six first yield values of this series, which do not overlap with yields of other series. They were used to estimate the total yields of these cluster ion series. Corresponding total yields are given in Table 1, together with decay constants k_m.

The series C_n^+, $(CO)C_n^+$ and $(CO)_2C_n^+$ present a similar decrease of yield with the increasing mass of the cluster (see Table 1).

3.3.5. C_n^- and O_n^- series

The lines in the negative ion spectrum are dominated by those of the C_n^- series and by the O^- peak. Fig. 7 displays the bar-spectrum of negative CO specific ions ejected from CO ice at $T = 25$ K. Again, clustering of carbon atoms C_n^- was observed and the oxygen atom O_n^- cluster series fits well masses 16, 32, 48, 64 and 80 u. Since (i) O_n neutrals are not pre-formed in CO ice; (ii) O_n^- secondary ions are observed; and (iii) O_n^+ are not clearly observed, the conclusion is that O^- is a better seed than O^+ for clustering oxygen atoms. To form the negative series, the electron capture process is competitive between carbon and oxygen atoms, since their electron affinities are similar (1.26 and 1.46 eV, respectively).

As four carbon atoms have the same mass as three oxygen atoms (within our mass resolution), the first cluster ion which

Table 1
Yields and decay constants of the positive cluster series $(CO)_mC_n^+$

	m_{bh} (u)	Y_{bh} (ions/impact)	Y_T (ions/impact)	k_m (u^{-1})
C_n^+	12	0.61	1.03	0.047
$(CO)C_n^+$	28	0.21	0.56	0.017
$(CO)_2C_n^+$	56	0.16	0.64	0.011
$(CO)_{m=1-17}^+$	28	0.030 (0.21)	0.17 (0.48)	0.007

m_{bh} is the mass of the band head ions, Y_{bh} the yield of the band head ions, Y_T the total yield of the cluster series and k_m the decay constant of the cluster series. For $((CO)_{m=1-17})^+$, the yields of the two first members of the series have been estimated by means of extrapolation using the data points $n = 3$–17. As seen in Fig. 8, the measured yields of CO^+ and $(CO)_2^+$ are much higher than expected from the trend of the $n > 2$ data points. The values given in brackets include the actual measured yields of these two ions.

can be assigned by two different combinations is the ion at $m = 48$ u: the corresponding peak can be either C_4^- or O_3^-. C_4^- is a typical secondary ion of organic samples (see, for instance, Wagner et al. [2]). In the survey article of Delitsky and Lane [17], it is pointed out that O_3 can be produced by ion beam irradiation of oxygen containing ices: this leads to the ambiguity between C^-_{n+4} and $C_nO_3^-$, as for masses 48, 60, 72, 84 u, and so on.

3.3.6. $(CO)C_n^-$ and $(CO_2)_nO^-$ series

CO^- ion has not been detected in this experiment, its mean life being too short compared to the acceleration time for secondary ions in the current setup. As in the case of positive ions, the negative ion spectrum exhibits CO specific mass lines only at mass numbers $m = 4(3i + 4j)$, with i and $j = 1, 2, 3, \ldots$, and the chemical designation of a given ion follows simply from possible combinations of C and O atoms. It is also observed that the unit CO appears often, which gives support to the designation of the $(CO)C_n^-$ series, i.e. masses 40, 52, 64, 76 and 88 u. Same observation holds for the unit CO_2, supporting the series $(CO_2)_nO^-$, i.e. masses 60, 104 and 148 u.

It is worthwhile to note that both C_n^- and $(CO_2)_n^-$ series also decay exponentially with the cluster mass and that the decay constant $k_m = 0.02\ u^{-1}$ is similar to those for the analyzed positive series.

3.4. Dependence of the positive CO series on the target temperature

Fig. 9 shows how the ion desorption yields of the $(CO)_m^+$, $(CO)C_n^+$ and $(CO)_2C_n^+$ series depend on the CO ice temperature near the fast sublimation condition. It is observed that this dependence is small until the dramatic decrease of the desorption yield at 30–32 K temperatures for all positive and negative ion clusters. Under such conditions, the sublimation rate is very high, gas phase collisions near the target should increase considerably and CO concentration tends to zero in the ice film. The target thickness decreases due to the fast CO sublimation but does not vanish because other gases (e.g. H_2O, N_2) are still frozen and are condensing from the chamber residual environment. Since the yields of all cluster members decrease proportionally as the sublimation point is approaching, the temperature increase appears to have quite a small influence on the decay constant of the ion series.

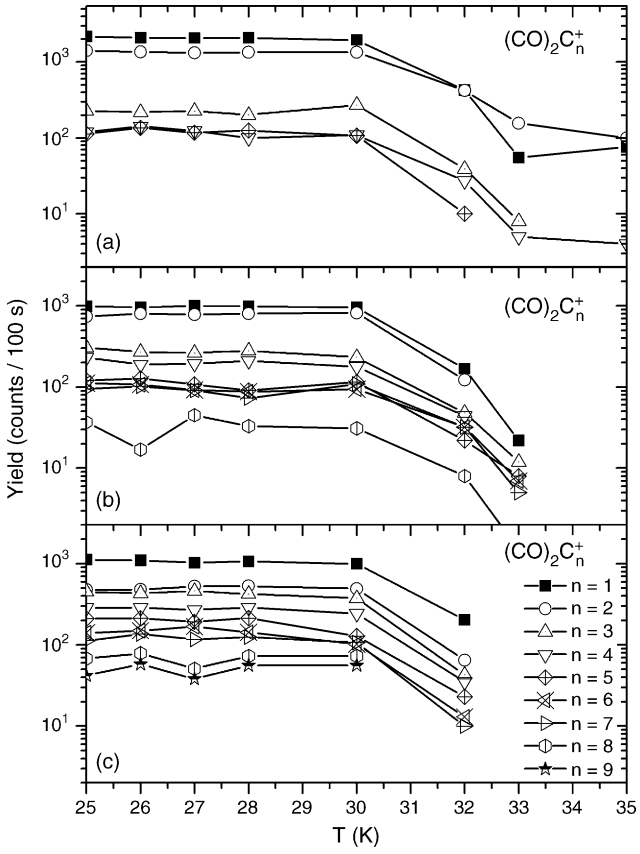

Fig. 9. The cluster yield dependence on the target temperature for the positive ion series: (a) $(CO)^+$; (b) $(CO)C_n^+$ and (c) $(CO_2)C_n^+$. Data for several nuclearities n are represented.

4. Discussion: the positive cluster ions

The electronic excitation of the CO ice surrounding the track of fission fragments is enormous: 65 MeV fission fragments release on the average 1200 eV/10^{15} at/cm^2. The corresponding total sputter yield was estimated by Johnson [15]: an equivalent of 2.4×10^5 CO molecules/impact. One reason for this relatively high sputter yield is the low effective intermolecular binding energy of 0.088 eV [15] of CO ice. The electronic excitation of the CO ice surrounding the track is primarily produced by the multi-charged projectiles and carried by δ-electrons up to about $R = 44$ nm deep into the ice. R is the projected range of these δ-electrons perpendicular to the track. The energy density ε is highest in the central core (radius ∼0.5 nm) and decreases in radial direction with the inverse square of distance [16]. A simple model [27] allows estimating the energy density in the central core: $\varepsilon_o = 60$ eV/molecule. This energy distributed to the electronic system dissipates in times of the order 10^{-15} s,—this means that, within this time, most of the positive ions created along the track become neutralized.

The ratio of charged to neutral particles observed for CO ice in the present experiments is about 1.2×10^{-5}. This is 1–2 orders of magnitude lower than the number of positive ions produced primarily in the ejected volume [15]. The process how the energy stored in the electronic system is transferred to the atomic system, i.e. to atomic motion, has been the subject of many theoretical investigations (see, for instance [28]). The electronic relaxation time seems to be too short to allow Coulomb explosion in the track core. Thus, many authors favor molecular expansion processes along the track, leading to destruction of the solid and close to the surface to ejection of more or less fragmented material. In accordance to the low intermolecular binding of CO ice and the high sputter yield, the assumption of hot plasma (which consists mainly of CO molecules) is certainly justified. The analysis of energy distributions of secondary ions ejected from organic solids by MeV heavy ions reveled temperatures higher than 3000 K [29].

4.1. C_n^+ cluster series

The spectral observation of C_n clusters proves that the highly excited material around the track must contain unbound carbon atoms, which condense in the expanding most probably gaseous sputtered material into monatomic carbon clusters or mixed $(CO)_mC_n$ clusters.

There are many ways to produce free carbon ion clusters [30]. In particular, they can be generated by laser vaporization of graphite [31] or by high frequency sparking between electrodes of graphite or carbon containing material [32], for which an explosive expansion of a highly excited gas volume occurs. We suggest that sputtering of CO ice induced by MeV heavy ions is a similar process. The explosive expansion is driven by a very high energy density in the central zone of the track, a density comparable to the two other processes. The time of expansion, i.e. the time elapsed until the rate of collisions approaches zero, is about 10^{-11} s,—certainly much shorter than the expansion time of the vapor plume emerging from the area of laser impact or electrical spark.

It is worthwhile to compare the C_n^+ cluster ion series measured in the present work with those reported in refs. [31,32]. As seen in Figs. 6 and 8, the C_n^+ series observed in the present work exhibits an exponential decrease superposed to a periodic intensity variation where the odd n correspond to local maxima. The negative C_n^- series has the opposite behavior: the even/odd periodicity presents maxima at even n (C_5^- and C_7^- have the same mass as CO_3^- and $(CO)_3^-$, respectively).

The steep decrease of cluster yields with increasing n is reported only for cluster production in sparks [32]: the mass distributions of carbon clusters produced by laser impact usually show up to $n=11$ an increase of intensity [31,33]. In the nuclear track plasma, the rate of associative collisions between carbon atoms or clusters is probably smaller than in the laser plume due to the relatively low density of carbon atoms. This density should be highest in the track core, where one expects complete destruction even of CO molecules. Further out the average C concentration is certainly much lower than the CO concentration. Another reason for the steep decrease of C_n^+ yields is that ions produced close to the surface undergo fewer collisions and have in addition, a larger chance to survive as charged species. C^+ has the highest yield of all ejected ions. Even multi charged species such as C^{2+}, N^{2+}, O^{2+} C^{3+} and O^{3+} were observed (see Fig. 2 insert) being generated by direct Coulomb interaction of the highly charged projectiles in the very first surface layers. As mentioned, by far most of the ions produced in deeper layers are lost by neutralization with electrons.

The odd/even periodicity of C_n^+ intensities observed for $n \leq 9$ is typical for all three production methods; the even/odd periodicity of C_n^- intensities has been observed in mass spectra obtained with sparks [32]. Theory (Hückel calculations [34]) predicts for linear C_n chains that positive odd clusters are more stable than even ones, and negative even clusters more stable than odd ones. These calculations were performed under the condition of thermal equilibrium, implying – for fission fragment bombardment – that the nuclear track plasma should have reached equilibrium before ejection of gas volume into vacuum. This seems to contradict the models in which the driving force is a repulsive expansion, a pressure pulse or a shock wave [35]. In the central core, where complete destruction supplies free carbon atoms, equilibrium (or at least a relatively low temperature) is eventually achieved, soon after pressure pulse propagation.

The C_n^+ distributions resulting from laser vaporization of graphite [31] show further intensity maxima at $n=11$, 15, 19 and 23, which are supposed to reflect monocyclic C_n ring structures [34]. As seen in Fig. 6, the mass line at $m=132$ u of C_{11}^+ (superposed to the $(CO)_3C_4^+$ one) stands out of the neighboring lines, and intensity maxima at $n=15$, 19, etc. are not clearly noticed. The spectra of neutral carbon clusters prepared by laser vaporization and cooled in a supersonic beam (see, for instance [33]) exhibit a pronounced even-n pattern, C_{2n}, for $n \geq 20$, candidate to the so-called fullerene structure. This spectral structure was also observed by MeV ion sputtering from a peculiar organic film, PVDF (polyvinylidene difluoride) [36]. A comparable assembly of mass lines in the mass range above $m \geq 480$ u was not found. According to the spectrum shown in Fig. 2, cut off at $m=482$ u, the yield of a C_{40}^+ ion should be $\leq 2 \times 10^{-4}$ ions/impact (see also Fig. 6). Regarding [36], the intensity of C_{40}^+ should be a factor 2 lower than that of C_{60}^+. Although the low mass part of [36] spectrum was not presented, the authors concluded from angular and energy distributions that the fullerene ion C_{60}^+ is ejected out of the central track core towards the direction of the incoming primary ion with a pronounced intensity. Formation of such a complex big molecule requires a track plasma which is relatively cold.

4.2. $(CO)_mC_n^+$ and $(CO)_m^+$ series

The $(CO)_m$ bulk molecules are expected to play a fundamental role in genesis of the $(CO)_mC_n^+$ and the $(CO)_m^+$ ion series The band heads of the mixed cluster ion series $(CO)_mC_n^+$ form a cluster series by themselves. The first two members of this series $(CO)_m^+$ have an outstanding high yield; – free CO is certainly the most abundant species of the nuclear track plasma – and $(CO)_2^+$ has a peculiarly high stability (binding energy 1.3 eV [37]). A supersonic CO jet contains after photon ionization a spectrum of $(CO)_m^+$ cluster ions with $(CO)_2^+$ having by far the highest intensity [37]. For $m \geq 3$, the $(CO)_m^+$ clusters are probably bound by electrostatic van der Waals forces. Since both ions, $(CO)^+$ and $(CO)_2^+$, are probably produced in parts of the track, where carbon atoms also exist, the series $(CO)C_n^+$ and $(CO)_2C_n^+$ are similar to the C_n^+ series. The fact that the decay constant k_m decreases with the mass of the band heads C_n^+, $(CO)^+$ and $(CO)_2^+$ might be explainable by their thermal velocities, whose lowest value occurs for the $(CO)_2^+$ [38].

For $m>2$, the yields of the series $(CO)_m^+$ decline much less with mass than those measured for the series C_n^+ and $(CO)_{m=1,2}C_n^+$, as illustrated in Fig. 8. A second observation is that the intensity of the attributed cluster ion series $(CO)_{m>2}C_n^+$ becomes progressively lower with an increasing cluster num-

ber m relative to the intensity of the band heads $(CO)_m^+$. For instance, the ratio of the yields of $(CO)_m^+$ and $(CO)_mC^+$ increases from 1.8 for $m=3$ to >6 for $m \geq 11$. The latter phenomenon could be caused by a decrease of the binding energy with m between $(CO)_m$ or $(CO)_m^+$ and carbon atoms or clusters. Such a decrease has been observed and calculated, for instance, for protonated ammonia clusters [39]. A second possibility is that the heavy $(CO)_m$ are produced further away from the central track core. This touches an important question, that is, knowing whether the mixed clusters are condensed from the gas phase, aggregating C and CO step by step, or if there exist $(CO)_m$ aggregates in the track plasma before condensation of carbon atoms. Such CO aggregates could be formed further away from the central core of the track, where the weakly bound CO solid is destructed, not necessarily only into single CO molecules, but also into CO aggregates.

Throughout this discussion bear in mind that, in the flux of about 2×10^5 particles sputtered particles from frozen CO per impact, the ratio of charged to neutral particles is extremely small ($\cong 8 \times 10^{-6}$); therefore, fast chemical reactions take place but thermodynamical equilibrium is not reached.

5. Conclusions

The present experimental investigation was addressed to the analysis of secondary ion mass spectra of condensed CO. The 65 MeV heavy ions, ^{252}Cf fission fragments, create along their track in the ice the so called nuclear track plasma, which expands near the surface into vacuum, where clusters are possibly produced by condensation from gas phase within 10^{-11} s. Other clusters, residues of the fractured solid, originate in the periphery of the impact site. The electronic sputtering of frozen CO has some peculiarities: its sputtering yield is five times higher than that of CO_2 ice; a very small fraction (0.0008%) of these particles is charged; the integrated yield of all negative CO specific ions is about 90 times smaller than that of the positive ions. The mass spectra of the positive SI show – apart from the primarily produced ions C^+, O^+ and CO^+ – a rich variety of cluster ions of type C_n^+ and $(CO)_mC_n^+$. The series with the highest yield has the index $m=2$ and probably consists of two sub-series: $(CO)_2C_n^+$ and $(CO_2)CC_n^+$. The relative yield of the observed series would depend on the ionization potential of the corresponding band heads which are very relevant to their formation probabilities.

The reactions leading to the C_n clusters require a high density of unbound carbon atoms in the nuclear track plasma. The main source for carbon atoms is the dissociation of CO, evidence for a substantial contribution of the reaction $CO + CO \rightarrow CO_2 + C$ has not been found. The yields of negative ions ejected from CO ice are unusually low.

The five most abundant cluster series, namely three positively and two negatively charged, decay exponentially with the cluster mass, all of them with about the same decay constant. It is concluded that this behavior is due to their common (statistical) process of formation. $(CO)_m^+$ may be partially constituted by preformed $(CO)_m$ neutral clusters. Periodic yield fluctuation over the exponential decay on n were observed for the series C_n^+ and C_n^-. They indicate thermalization of the track plasma at the time of cluster formation, i.e. condensation in gas-phase.

Acknowledgements

The authors would like to acknowledge the Brazilian Agencies CNPq, Fapesp and Faperj for their partial support. P. Iza acknowledges CLAF for his scholarship.

References

[1] E.F. da Silveira, C.D. McAfee, D.L. Cocke, D.G. Naugle, D. Sun, E.A. Schweikert, Int. J. Mass Spec. Ion Proc. 91 (1989) R5.
[2] M. Wagner, K. Wien, B. Curdes, E.R. Hilf, Nucl. Instum. Meth. B 82 (1993) 362.
[3] K. Wien, A. Spieth, Rapid Commun. Mass Spectrom. 9 (1995) 221.
[4] K. Wien, C.S.C. de Castro, Nucl. Instrum. Meth. B 146 (1998) 178.
[5] R.L. Betts, E.F. da Silveira, E.A. Schweikert, Int. J. Mass Spec. Ion Proc. 145 (1995) 9.
[6] V.M. Collado, L.S. Farenzena, C.R. Ponciano, E.F. da Silveira, K. Wien, Surf. Sci. 569 (2004) 149.
[7] L.S. Farenzena, V.M. Collado, C.R. Ponciano, E.F. da Silveira, K. Wien, Int. J. Mass Spec. Ion Proc. 243 (2005) 85–93.
[8] C.R. Ponciano, L.S. Farenzena, V.M. Collado, E.F. da Silveira, K. Wien, Int. J. Mass Spec. Ion Proc. 244 (2005) 41–49.
[9] D.B. Chrisey, W.L. Brown, J.W. Boring, Surf. Sci. 225 (1989) 130.
[10] R.L. Hudson, M.H. Moore, J. Geophys. Res. 106 (2001) 33, 275–33, 284; see also J. Geophys. Res. 96 (1991) 17, 541.
[11] R.A. Haring, P. Pedrys, D.J. Oostra, A. Haring, A.E. de Vries, Nucl. Instrum. Meth. B5 (1984) 476.
[12] R.D. Macfarlane, D.F. Torgerson, Science 191 (1976) 920.
[13] L.C. Northcliffe, R.F. Schilling, Nuclear Data Tables, in: K. Way (Ed.), vol. A7 (3–4), 1970.
[14] K. Wien, Nucl. Instrum. Meth. B 131 (1997) 38–54.
[15] R.E. Johnson, Energetic Charged Particle Interactions with Atmospheres and Surfaces, Springer–Verlag, Heidelberg, 1990.
[16] E.J. Kobetich, R. Katz, Phys. Rev. 170 (1968) 391.
[17] M.L. Delitsky, A.L. Lane, J. Geophys. Res. 102 (1997) 385.
[18] G.M. Lancaster, F. Honda, J.W. Rabalais, J. Am. Chem. Soc. 79 (1979) 1951.
[19] T. Matsuo, T. Tonuma, H. Kumagai, H. Tawara, J. Chem. Phys. 101 (1994) 5356.
[20] R. Martinez, C.R. Ponciano, L.S. Farenzena, P. Iza, M.G.P. Homem, A. Naves de Brito, K. Wien, E.F. da Silveira, submitted for publication.
[21] V.M. Collado, F.A. Fernandez-Lima, C.R. Ponciano, M.A.C. Nascimento, L. Velázquez, E.F. da Silveira, Phys. Chem. Chem. Phys. 7 (2005) 1971–1976.
[22] R.L. Johnston, Atomic and Molecular Clusters, Taylor & Francis, London, 2002.
[23] A. Wucher, M. Wahl, Nucl. Instrum. Meth. B 115 (1996) 581.
[24] A.V. Hamza, T. Schenkel, A.V. Barnes, Eur. Phys. J. D 6 (1999) 83.
[25] L.E. Rehn, R.C. Birtcher, S.E. Donnelly, P.M. Baldo, L. Funk, Phys. Rev. Lett. 87 (2001) 207601.
[26] C. Staudt, A. Wucher, Phys. Rev. B 66 (2002) 075419.
[27] C.C. Watson, T.A. Tombrello, Radiat. Eff. 89 (1985) 263.
[28] K. Wien, Nucl. Instrum. Meth. B 65 (1992) 149.
[29] G. Betz, K. Wien, Int. J. Mass Spec. Ion Proc. 140 (1994) 1.
[30] Cluster Ions, in: C.-Y. Ng, T. Baer, I. Powis (Eds.), Wiley Series in Ion Chemistry and Physics, John Wiley & Sons, 1993.
[31] N. Fürstenau, Z. Fresenius, Anal. Chem. 308 (1981) 201.
[32] H. Hintenberger, J. Franzen, K.D. Schuy, Z. Naturforsch. 18a (1963) 1236.
[33] E.A. Rohlfing, D.M. Cox, A. Kaldor, J. Chem. Phys. 81 (7) (1984) 3322.

[34] K.S. Pitzer, E. Clementi, J. Am. Chem. Soc. 21 (1959) 4477.
[35] R.E. Johnson, B.U.R. Sundqvist, A. Hedin, D. Fenyö, Phys. Rev. B 40 (1) (1989) 49;
I.S. Bitensky, E.S. Parilis, Nucl. Instrum. Meth. B 21 (1987) 26.
[36] G. Brinkmalm, P. Demirev, D. Fenyö, P. Håkansson, J. Kopniczky, B.U.R. Sundqvist, Phys. Rev. B 47 (12) (1993) 7560.
[37] K. Norwood, J.-H. Guo, G. Luo, C.Y. Ng, J. Chem. Phys. 90 (11) (1989) 6026.
[38] G.P. Können, A. Tip, A.E. de Vries, Radiat. Eff. 26 (1975) 23.
[39] S. Wei, W.B. Tzeng, A.W. Castleman Jr., J. Chem. Phys. 93 (1990) 2506.